J|A|C|S ARTICLES

Published on Web 07/21/2010

Simultaneous Discrimination of Handedness and Diameter of Single-Walled Carbon Nanotubes (SWNTs) with Chiral Diporphyrin Nanotweezers Leading to Enrichment of a Single Enantiomer of (6,5)-SWNTs

Feng Wang,[†] Kazunari Matsuda,[‡] A. F. M. Mustafizur Rahman,[#,†] Xiaobin Peng,[⊥,†] Takahide Kimura,[†] and Naoki Komatsu*[,†]

Department of Chemistry, Shiga University of Medical Science, Seta, Otsu 520-2192, Japan, and Institute for Chemical Research, Kyoto University, Gokasho, Uji, Kyoto 611-0011, Japan

Received May 24, 2010; E-mail: nkomatsu@belle.shiga-med.ac.jp

Abstract: Separation of single-walled carbon nanotubes (SWNTs) according to their handedness has been attracting growing interest. Our methodology to separate the enantiomers of SWNTs is based on molecular recognition with chiral diporphyrin nanotweezers. Herein, we report novel nanotweezers **1** consisting of two chiral porphyrins and phenanthrene in between. These nanotweezers **1** are rationally designed to discriminate diameter and handedness simultaneously by taking into account the relationship between the (*n*, *m*) selectivity and the structures of previously reported chiral nanotweezers. Owing to the relatively narrow cleft made by two porphyrins, the nanotweezers **1** showed high selectivity toward (6,5)-SWNTs possessing the smallest diameter among the major components of CoMoCAT−SWNTs. In addition, the chiral diporphyrin **1** discriminated the left- and right-handed structures of (6,5)-SWNTs, providing high enantiomeric excess (67% ee on the basis of the (6,5)-SWNTs with high optical purity recently reported by Weisman). In conclusion, only the single stereoisomer of (6,5)-SWNTs was highly enriched through the extraction of CoMoCAT−SWNTs with phenanthrene-bridged chiral diporphyrin nanotweezers **1**.

1. Introduction

A single-walled carbon nanotube (SWNT) has a cylindrical structure consisting of a wrapped graphene sheet. The structure is defined by the roll-up index, (*n*, *m*), which is connected to the origin, (0,0), by rolling up the graphene map (see Figure 2d). While SWNTs with (*n*, *n*) and (*n*, 0), designated as armchair and zigzag, respectively, are achiral, all the other structures are chiral and, therefore, each chiral SWNT is either of the enantiomers defined as *M* and *P*.[1] As-produced SWNTs include both enantiomers in equal amounts and, therefore, are optically inactive. In addition, various types of (*n*, *m*)-SWNTs are contained in the SWNTs, even in those possessing a limited diameter range (see Table 1).

Since the electrical and optical properties of SWNTs are closely correlated to their structures, structural control of SWNTs is important for their applications.[2] Extensive investigations have been made in pursuit of selective synthesis and separation of SWNTs with specific structural or electrical properties. While great progress has been made recently on the selective synthesis of metallic and semiconducting (M/S) SWNTs,[3,4] SWNTs have to be separated to obtain a specific (*n*, *m*) structure as a pure form.[1,5−9] The (*n*, *m*)-separation

Table 1. Change in Distances between Two Zn Atoms in Diporphyrin Nanotweezers **1** before and after Complexation with SWNTs[a]

major components in CoMoCAT	diameter (nm)	roll-up angle (deg)	Zn−Zn distance (nm)
—	—	—	1.05
(6,4)	0.69	23.4	1.18
(9,1)	0.76	5.2	1.20
(7,4)	0.75	21.1	1.20
(6,5)	0.76	27.0	1.20
(8,3)	0.78	15.3	1.21
(7,5)	0.83	24.5	1.22
(8,4)	0.84	19.1	1.22
(8,5)	0.89	22.4	1.23
(7,6)	0.90	27.5	1.24

[a] Molecular mechanics calculation.

* Corresponding author.
† Shiga University of Medical Science.
‡ Kyoto University.
⊥ Current address: Institute of Polymer Optoelectronic Materials & Devices, Key Laboratory of Specially Functional Materials and Advanced Manufacturing Technology (Ministry of Education), South China University of Technology, Guangzhou 510640, China.
On leave from Department of Applied Chemistry and Chemical Engineering, University of Dhaka, Dhaka 1000, Bangladesh.

(1) Komatsu, N.; Wang, F. *Materials* **2010**, *3*, 3818–3844.
(2) Baughman, R. H.; Zakhidov, A. A.; Heer, W. A. d. *Science* **2002**, *297*, 787–792.
(3) Harutyunyan, A. R.; Chen, G.; Paronyan, T. M.; Pigos, E. M.; Kuznetsov, O. A.; Hewaparakrama, K.; Kim, S. M.; Zakharov, D.; Stach, E. A.; Sumanasekera, G. U. *Science* **2009**, *326*, 116–120.
(4) Hong, G.; Zhang, B.; Peng, B.; Zhang, J.; Choi, W. M.; Choi, J.-Y.; Kim, J. M.; Liu, Z. *J. Am. Chem. Soc.* **2009**, *131*, 14642–14643.
(5) Hersam, M. C. *Nat. Nanotechnol.* **2008**, *3*, 387–394.
(6) Campidelli, S.; Meneghetti, M.; Prato, M. *Small* **2007**, *3*, 1672–1676.
(7) Krupke, R.; Hennrich, F. In *Chemistry of carbon nanotubes*; Basiuk, V. A., Basiuk, E. V., Eds.; American Scientific Publishers: Stevenson Ranch, CA, 2008; Vol. 3, pp 129−139.
(8) Krupke, R.; Hennrich, F. *Adv. Eng. Mater.* **2005**, *7*, 111–116.

10.1021/ja1044677

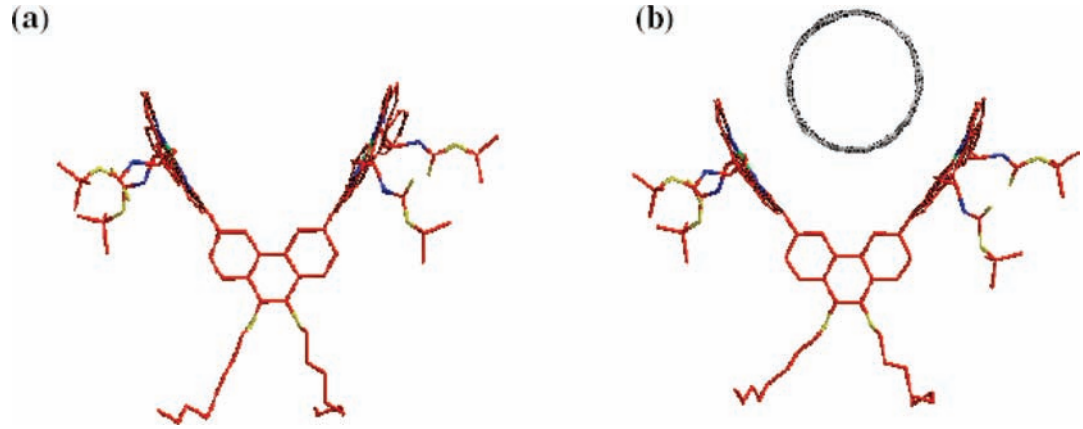

Figure 1. Computer-generated molecular models of (*R*)-**1** (a) and the complex of (*R*)-**1** with (*P*)-(6,5)-SWNTs (b).

Scheme 1. Synthesis of Chiral Diporphyrin Nanotweezers via Suzuki-Miyaura Coupling Reaction

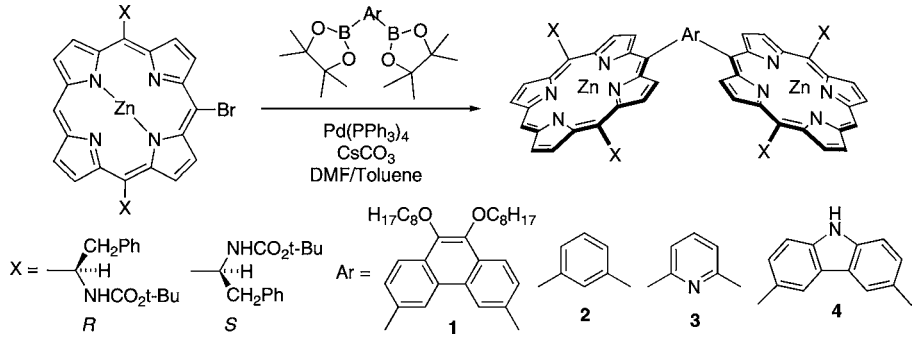

methods reported so far include density gradient ultracentrifugation (DGU),[10–14] chromatography,[15–18] polymer-assisted selective extraction,[10,19–23] and electrochemical doping.[24–26] Relatively small molecules have also been utilized for separation of SWNTs through recognition of a specific (*n*, *m*) structure.[19,20,27,28]

Recently, handedness, another structural feature of carbon nanotubes, has been attracting significant interest.[29] Separation of left- and right-handed structures giving optically active SWNTs has been realized by the selective extraction with chiral porphyrins developed by us,[30–33] DGU with sodium cholate (chiral detergent) by Hersam,[34] and sodium cholate/sodium dodecylsulfonate (SDS) by Weisman.[14] While the DGU method provided almost pure (6,5)-SWNTs with high optical purity,[14,34] we obtained optically active forms of a few (*n*, *m*) structures as a mixture.[30–33] In continuation of our effort to improve discrimination ability of our diporphyrin nanotweezers, the rationally designed chiral diporphyrin nanotweezers **1**, shown in Figure 1 and Scheme 1, were found to exhibit high discrimination ability toward diameter and handedness simultaneously. This enabled enrichment of either left- or right-handed stereoisomer of (6,5)-SWNTs through the extraction of CoMoCAT−SWNTs (SWNTs prepared by chemical vapor deposition (CVD) process using a silica-supported Co−Mo catalyst)[35] with our designed nanotweezers **1**.

2. Results and Discussion

In the molecular design of the present nanotweezers **1**, we reconsidered the following relationships between the structures of the nanotweezers designed previously and the types of the SWNTs extracted selectively:[30–33] (1) the chiral nanotweezers **2**−**4** bearing stereogenic centers adjacent to the porphyrin rings

(9) Papadimitrakopoulos, F.; Ju, S.-Y. *Nature* **2007**, *450*, 486–487.
(10) Stürtl, N.; Hennrich, F.; Lebedkin, S.; Kappes, M. M. *J. Phys. Chem. C* **2009**, *113*, 14628–14632.
(11) Arnold, M. S.; Green, A. A.; Hulvat, J. F.; Stupp, S. I.; Hersam, M. C. *Nature Nanotechnol.* **2006**, *1*, 60–65.
(12) Arnold, M. S.; Stupp, S. I.; Hersam, M. C. *Nano Lett.* **2005**, *5*, 713–718.
(13) Green, A. A.; Hersam, M. C. *Nano Lett.* **2008**, *8*, 1417–1422.
(14) Ghosh, S.; Bachilo, S. M.; Weisman, R. B. *Nat. Nanotechnol.* **2010**, *5*, 443–450.
(15) Tu, X.; Manohar, S.; Jagota, A.; Zheng, M. *Nature* **2009**, *460*, 250–253.
(16) Zhang, L.; Tu, X.; Welsher, K.; Wang, X.; Zheng, M.; Dai, H. *J. Am. Chem. Soc.* **2009**, *131*, 2454–2455.
(17) Zhang, L.; Zaric, S.; Tu, X.; Wang, X.; Zhao, W.; Dai, H. *J. Am. Chem. Soc.* **2008**, *130*, 2686–2691.
(18) Zheng, M.; Semke, E. D. *J. Am. Chem. Soc.* **2007**, *129*, 6084–6085.
(19) Marquis, R.; Greco, C.; Sadokierska, I.; Lebedkin, S.; Kappes, M. M.; Michel, T.; Alvarez, L.; Sauvajol, J.-L.; Meunier, S.; Mioskowski, C. *Nano Lett.* **2008**, *8*, 1830–1835.
(20) Marquis, R.; Kulikiewicz, K.; Lebedkin, S.; Kappes, M. M.; Mioskowski, C.; Meunier, S.; Wagner, A. *Chem.—Eur. J.* **2009**, *15*, 11187–11196.
(21) Nish, A.; Hwang, J.-Y.; Doig, J.; Nicholas, R. J. *Nat. Nanotechnol.* **2007**, *2*, 640–646.
(22) Hwang, J.-Y.; Nish, A.; Doig, J.; Douven, S.; Chen, C.-W.; Chen, L.-C.; Nicholas, R. J. *J. Am. Chem. Soc.* **2008**, *130*, 3543–3553.
(23) Chen, F.; Wang, B.; Chen, Y.; Li, L.-J. *Nano Lett.* **2007**, *7*, 3013–3017.
(24) Kato, Y.; Niidome, Y.; Nakashima, N. *Angew. Chem., Int. Ed.* **2009**, *48*, 5435–5438.
(25) Kalbác, M.; Kavan, L.; Dunsch, L. *J. Am. Chem. Soc.* **2009**, *131*, 4529–4534.
(26) Niyogi, S.; Boukhalfa, S.; Chikkannanavar, S. B.; McDonald, T. J.; Heben, M. J.; Doorn, S. K. *J. Am. Chem. Soc.* **2007**, *129*, 1898–1899.
(27) Ju, S.-Y.; Doll, J.; Sharma, I.; Papadimitrakopoulos, F. *Nat. Nanotechnol.* **2008**, *3*, 356–362.
(28) Ogunro, O. O.; Wang, X.-Q. *Nano Lett.* **2009**, *9*, 1034–1038.
(29) S.-Castillo, A.; Noguez, C. *J. Phys. Chem. C*, **2010**, *114*, 9640–9644.
(30) Peng, X.; Komatsu, N.; Bhattacharya, S.; Shimawaki, T.; Aonuma, S.; Kimura, T.; Osuka, A. *Nat. Nanotechnol.* **2007**, *2*, 361–365.
(31) Peng, X.; Komatsu, N.; Kimura, T.; Osuka, A. *J. Am. Chem. Soc.* **2007**, *129*, 15947–15953.

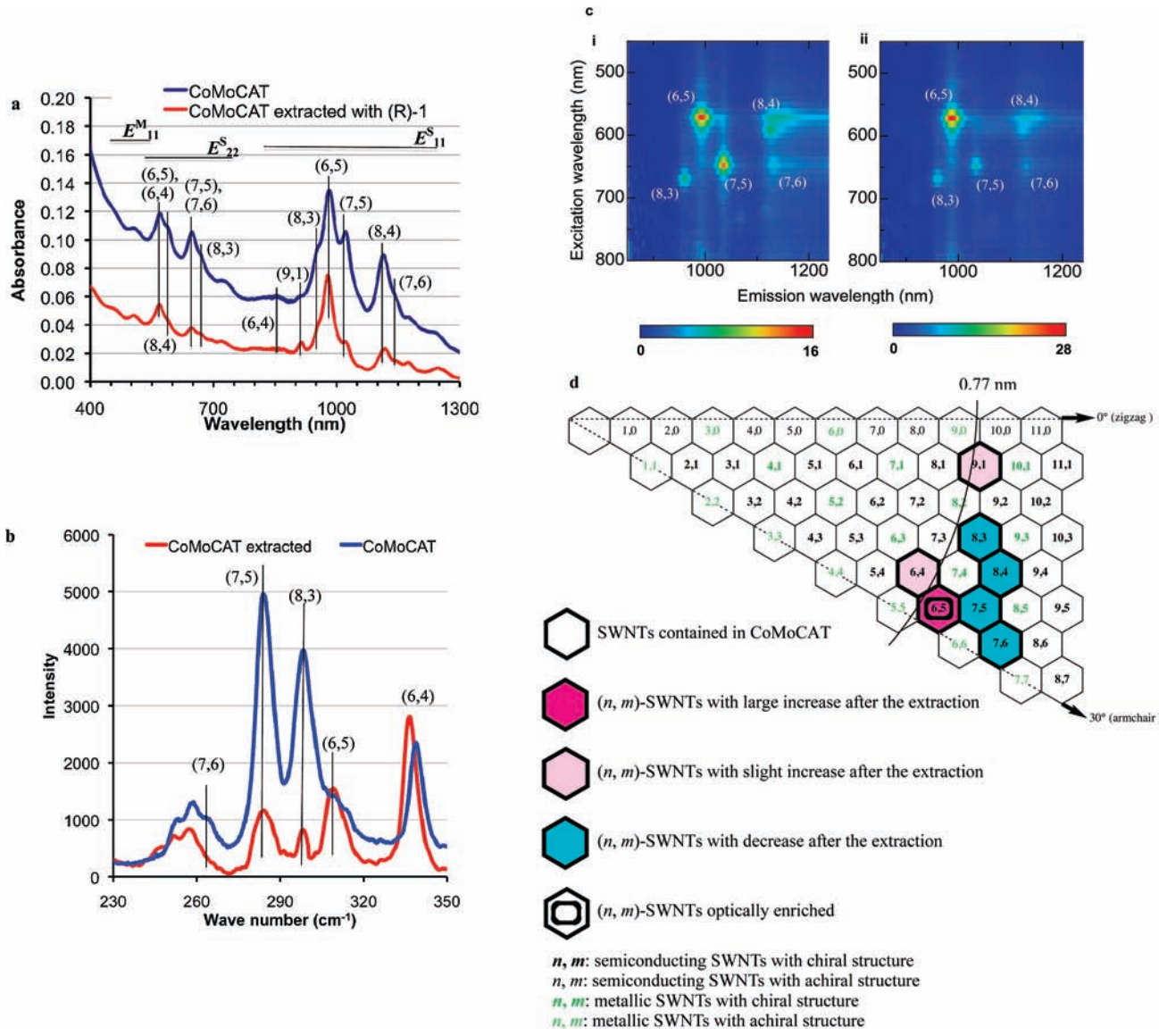

Figure 2. (a) Absorption and (b) Raman (excitation wavelength: 633 nm) spectra of CoMoCAT before and after extraction with (*R*)-**1**. (c) Photoluminescence (PL) spectra of CoMoCAT (i) before and (ii) after extraction with (*R*)-**1**. The scale intensity is shown below the spectra. (d) Summary of increase and decrease of semiconducting (*n*, *m*)-SWNTs in abundance upon extraction of CoMoCAT with (*R*)-**1**. The diameter of a (*n*, *m*)-SWNT is corresponding to the length between the origin (the point where the two dotted lines crossed) and the (*n*, *m*) (left-up vertex in the (*n*, *m*) hexagon) in the map.

(see Scheme 1) discriminate left- and right-handed structures to provide optically active SWNTs, (2) the chiral nanotweezers also recognize structural features of SWNTs (diameter and/or (*n*, *m*) structure) other than handedness, (3) the type of SWNTs selectively extracted is changed by modifying the structure of the nanotweezers, namely the length of the spacer and the angle of the two porphyrins, and (4) nanotweezers **4** with the longer spacer and narrower angle exhibits better (*n*, *m*) selectivity than **2** and **3**, probably due to deep accommodation of SWNTs in the cleft. By taking the above (1)−(4) into account, the novel nanotweezers **1** have been designed to strictly discriminate the diameter of SWNTs together with the handedness.

The tweezers **1** include phenanthrene as a spacer (see Scheme 1 and Figure 1a) to make the dihedral angle (56°) narrower than those in the previous nanotweezers **2**−**4**[33] including *m*-phenylene (111°),[30] 2,6-pyridylene (94°),[31] and 3,6-carbazolylene (74°), respectively.[32] The molecular modeling depicted in Figure 1a shows that (6,5)-SWNTs having the smallest diameter among the major components in CoMoCAT−SWNTs are tweezed in the narrow cleft of **1**. The degree of the deformation of the tweezer structure, as estimated from the Zn−Zn distance in Table 1, is less in the (6,5)-SWNT/nanotweezers complex than in the complexes with the major components of CoMoCAT having larger diameters; (8,3), (7,5), (8,4) (8,5), and (7,6)-SWNTs (see Figure 2d). Therefore, (6,5)-SWNTs are expected to form a more stable complex with **1** than the SWNTs with larger diameters. This is considered to lead to selective extraction of (6,5)-SWNTs, because (6,5)-SWNTs have the smallest diameter among the major components of CoMoCAT.

(32) Peng, X.; Komatsu, N.; Kimura, T.; Osuka, A. *ACS Nano* **2008**, *2*, 2045–2050.
(33) Peng, X.; Wang, F.; Bauri, A.; Rahman, A. F. M. M.; Komatsu, N. *Chem. Lett.*, in press.
(34) Green, A. A.; Duch, M. C.; Hersam, M. C. *Nano Res.* **2009**, *2*, 69–77.
(35) Bachilo, S. M.; Balzano, L.; Herrera, J. E.; Pompeo, F.; Resasco, D. E.; Weisman, R. B. *J. Am. Chem. Soc.* **2003**, *125*, 11186–11187.

The diporphyrin nanotweezers **1** were synthesized through Suzuki−Miyaura coupling reaction as shown in Scheme 1. When the porphyrin boronate was reacted with the dibromoarene as reported previously,[30–33] the yield of the diporphyrin **1** was relatively low (less than 10% yield) and instead a large amount of a monoporphyrin was recovered. However, the yield increased remarkably to ~80% in the reverse combination of the bromide and boronate as shown in Scheme 1. These compounds were fully identified with ESI-MS, absorption, and ^{1}H NMR spectoroscopies as well as elemental analysis. The details of the synthetic procedure and the analytical data are described in the Experimental Section and the Supporting Information.

In the extraction, CoMoCAT (10 mg) and **1** (10 mg) in methanol (40 mL) were bath-sonicated at 20 °C for 16 h and centrifuged at 50400*g* for 3 h. The formation of the complex was confirmed by red shifts in the absorption spectra, quenching of the fluorescence from the porphyrin, and enhanced Cotton effects in circular dichroism (CD) spectra as shown in Figure S1 in the Supporting Information.[36] After concentration of the supernatant, the diporphyrin was washed out from the complex with pyridine and THF. This process is important to obtain pristine SWNTs and avoid induced CD.[37] Since removal of the detergent and additives following the separation is considered not to be facile in the DGU method, this washing process is one of the characteristics of our methodology as well as the flexibility in the molecular design of the host molecules mentioned above. The solid sample was subjected to Raman spectroscopy to compare the relative (*n*, *m*) abundance of SWNTs before and after the extraction. After the sample was dissolved in D_2O with the aid of achiral detergent (sodium dodecylbenzenesulfonate, SDBS), absorption, photoluminescence (PL), and CD spectra were measured to evaluate the enrichments in (*n*, *m*) and optical purity of SWNTs.

After the extraction of CoMoCAT with **1**, (6,5)-SWNTs were remarkably enriched as shown in both E^S_{11} and E^S_{22} (electronic transitions parallel to the nanotube axis in semiconducting SWNTs)[29] regions in the absorption spectra (Figure 2a), while the contents of (8,3), (7,5), (8,4), and (7,6) were decreased relatively. The increase of (9,1) is also clearly recognized at 910 nm in the absorption spectra (Figure 2a), although the absorbance is relatively small. An almost consistent result is obtained in the Raman spectra at an excitation of 633 nm as shown in Figure 2b. The peak intensity of (6,5) enhanced after extraction, while those of (7,5), (7,6), and (8,3) largely decreased. (6,4)-SWNTs were also enriched slightly after the extraction, probably because **1** can also form a complex with (6,4) having a smaller diameter than (6,5) as indicated in Table 1 and Figure 2d. Since the relative increase of (6,4) is not clear in the absorption spectra (Figure 2a), the actual content of (6,4) may be negligible both before and after the extraction. PL spectra shown in Figure 2c further support the above conclusion of relative increase of (6,5) and relative decrease of (8,3), (7,5), (8,4), and (7,6). The peaks of (9,1) and (6,4) are not clearly detected, probably because of their very low abundance.

The relative increase and decrease of the major semiconducting (*n*, *m*) components included in CoMoCAT−SWNTs are summarized in the map shown in Figure 2d. It is obvious from the map that the designed chiral nanotweezers **1** discriminate the diameter of SWNTs; diameters less than 0.77 nm (the line drawn in the map), including (6,5), (9,1), and (6,4), are enriched, while those more than 0.77 nm, including (8,3), (7,5), (8,4), and (7,6), are relatively decreased. These results indicate that the complex of nanotweezers **1** with SWNTs becomes unstable, once the diameter of the SWNTs exceeds 0.77 nm. (6,5)- and (9,1)-SWNTs having 0.76 nm in diameter may be the upper limit in (*n*, *m*), with which **1** can form a stable complex. Since (6,5)-SWNTs are the only major component in the CoMoCAT−SWNTs having less than 0.77 nm in diameter, only the (6,5)-SWNTs are considered to be enriched largely through the extraction with **1** from the mixture of SWNTs.

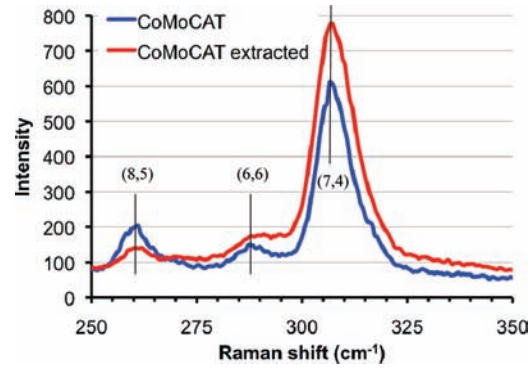

Figure 3. Raman spectra of CoMoCAT before and after extraction with **1** at an excitation of 488 nm.

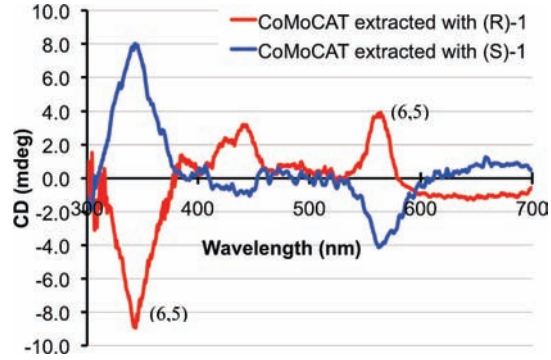

Figure 4. CD spectra of SWNTs extracted with (*R*)- and (*S*)-**1**.

The metallic components of CoMoCAT were detected in Raman spectra at an excitation of 488 nm as shown in Figure 3. A relative increase for (7,4) and relative decease for (8,5) are observed among the metallic SWNTs.[38] This result also supports that the nanotweezers **1** discriminated the diameter of CoMoCAT−SWNTs as described above, because (7,4)- and (8,5)-SWNTs have 0.75 and 0.89 nm diameters, respectively, as shown in Table 1 and Figure 2d. The semiconducting-to-metallic ratio is reported to be 11:1 in CoMoCAT.[38] The ratio is not considered to change so much after the extraction, judging from the E^M_{11} region in the absorption spectra (Figure 2a). Since the amount of the metallic SWNTs are much smaller than that of the semiconducting SWNTs, we can conclude that the (*n*, *m*) selectivity is determined by the relative abundance of the semiconducting (*n*, *m*)-SWNTs before and after the extraction, as illustrated in Figure 2d.

In addition to the (6,5) enrichment mentioned above, the SWNTs extracted with (*R*)- and (*S*)-**1** gave symmetrical CD

(36) Backes, C.; Schmidt, C. D.; Rosenlehner, K.; Hauke, F.; Coleman, J. N.; Hirsch, A. *Adv. Mater.* **2010**, *22*, 788–802.
(37) Dukovic, G.; Balaz, M.; Doak, P.; Berova, N. D.; Zheng, M.; Mclean, R. S.; Brus, L. E. *J. Am. Chem. Soc.* **2006**, *128*, 9004–9005.
(38) Jorio, A.; Santos, A. P.; Ribeiro, H. B.; Fantini, C.; Souza, M.; Vieira, J. P. M.; Furtado, C. A.; Jiang, J.; Saito, R.; Balzano, L.; Resasco, D. E.; Piementa, M. A. *Phys. Rev. B* **2005**, *72*, 075207.

Table 2. Comparison of Enantiomeric Excess (ee) of (6,5)-SWNTs Resolved in the Three Groups

authors	method[a]	CD_{raw} (mdeg)[b]	L_{CD} (cm)[c]	A_{E22}[d]	L_{abs} (cm)[e]	CD_{norm} (mdeg)[f]	ee (%)[g]
Ghosh, Weisman[h]	DGU	20	1.0	0.55	1.0	36	100
Green, Hersam[i]	DGU	13	1.0[j]	0.60	1.0[j]	22	61
Wang, Komatsu[k]	molecular recognition	4.0	10	0.017[l]	1.0	24[m]	67

[a] DGU: density gradient ultracentrifugation. [b] Reported CD intensity of (6,5)-SWNTs at the E_{22} region. [c] Optical path length in CD spectral measurement. [d] Reported absorbance of (6,5)-SWNTs at the E_{22} region. [e] Optical path length in absorption spectral measurement. [f] CD_{norm} was calculated according to the equation 1. [g] The ee (%) was calculated from the CD_{norm} reported in the Weismans's paper. [h] Reference 14. [i] Reference 34. [j] Private communication. [k] This work. [l] Figure 2a. [m] Figure 4.

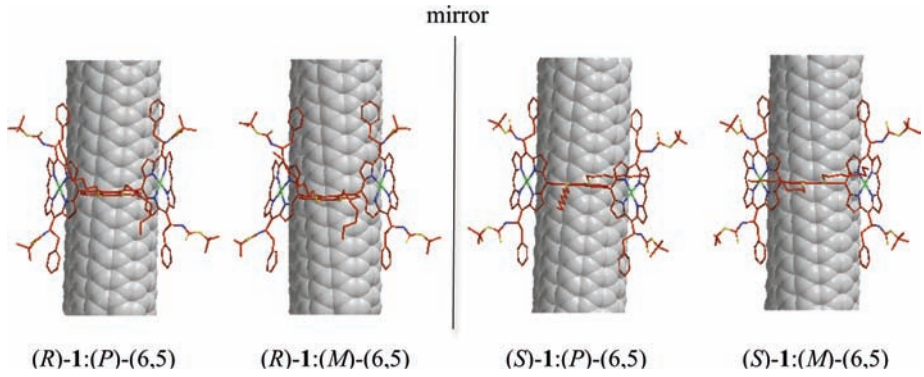

Figure 5. Computer-generated complex structures of (*R*)- and (*S*)-**1** with (*P*)- and (*M*)-(6,5)-SWNTs.

spectra of the (6,5)-SWNTs after their dissolvation, as shown in Figure 4. The CDs corresponding to the E^S_{22} and E^S_{33} of the (6,5)-SWNTs are clearly found at 566 and 344 nm, respectively. Another CD observed around 430 nm may be due to the E^S_{32} (electronic transitions perpendicular to the nanotube axis)[29] of (6,5)-SWNTs. No chiral metallic SWNTs, such as (7,4)-SWNTs detected on Raman spectra (Figure 3), show CD signals.[38] The whole spectra are in good agreement with both experimental and calculated spectra of (6,5)-SWNTs reported so far, although E^S_{12} of (6,5)-SWNTs are not clearly observed around 650 nm in Figure 4.[14,29,31,34] This indicates that only (6,5)-SWNTs give rise to optical activity, while no other (*n*, *m*)-SWNTs exhibit clear CD signals because of their low optical activity and/or low abundance. In conclusion, optical enrichment of (6,5)-SWNTs occurred simultaneously together with the (*n*, *m*) enrichment of (6,5). In other words, the single structure of SWNTs, one enantiomer of the specific (*n*, *m*), was enriched through molecular recognition using chiral nenotweezers **1**. The single enantiomer enrichment has been accomplished so far only by the DGU method.[14,34]

In order to compare the optical purity of the extracted (6,5)-SWNTs with those reported by Hersam[34] and Weisman,[14] the CD spectra shown in Figure 4 were normalized according to the following equation 1;

$$CD_{norm} = (CD_{raw}/L_{CD})/(A_{E22}/L_{abs}) \quad (1)$$

where CD_{raw}, CD_{norm}, A_{E22}, L_{CD}, and L_{abs} indicate CD intensities (mdeg) before and after normalization, abosorbance at 566 nm in the E_{22} transition, and the optical path length (cm) in the CD and absorption spectroscopies, respectively. The enantiomeric excess (ee) of (6,5)-SWNTs is calculated on the basis of the recent result reported by Weisman,[14] because (6,5)-SWNTs are optically resolved into two well-separated bands by DGU and, therefore, are considered to have very high optical purity. These results are summarized in Table 2. Surprisingly, 67% ee was obtained through the optical resolution with chiral nanotweezers **1**. The ee of our sample is close to that obtained by the DGU method in Hersam's group. The result shows that discrimination ability of our chiral nanotweezers to the handedness of (6,5)-SWNTs is unexpectedly high.

The preference of the chiral tweezers to the (*M*)- and (*P*)-stereoisomers[1] of (6,5)-SWNTs is estimated by molecular mechanics simulations shown in Figure 5. In the case of the complexes between **1** and (6,5)-SWNTs, the enantiomers, (*R*)-**1**: (*P*)-(6,5) and (*S*)-**1**: (*M*)-(6,5), are found to be more stable than the diasteromers, (*R*)-**1**: (*M*)-(6,5) and (*S*)-**1**: (*P*)-(6,5), respectively. These results suggest that the more stable complex (*R*)-**1**: (*P*)-(6,5) or (*S*)-**1**: (*M*)-(6,5) is present more in the supernatant, while the less stable complex (*R*)-**1**: (*M*)-(6,5) or (*S*)-**1**: (*P*)-(6,5) exists more in the precipitates. From the molecular modeling, (*P*)- and (*M*)-(6,5)-SWNTs are considered to be enriched by use of (*R*)- and (*S*)-**1**, respectively. The ratio between (*M*)- and (*P*)-(6,5)-SWNTs are calculated from the ee in Table 2 to be 17:83 and 83:17 after the extraction with (*R*)- and (*S*)-**1**, respectively.

3. Conclusion

We rationally designed the chiral nanotweezers **1**, consisting of phenanthrene spacer and two chiral porphyrins, for descrimination of the handedness and diameter of SWNTs simultaneously. The smaller dihedral angle (56°) made by two porphyrins are effective to selectively tweeze out (6,5)-SWNTs possessing the smallest diameter among the major components of CoMoCAT−SWNTs. In addition, only (6,5)-SWNTs exhibit CD, indicating that the single enantiomer of (6,5)-SWNTs is enriched through the molecular recognition with **1**. The enantiomeric excess (ee) of the extracted (6,5)-SWNTs is estimated to be 67% on the basis of the previously reported CD intensity and the corresponding absorbance.

4. Experimantal Section

Materials. CoMoCAT was purchased from SouthWest Nano-Technologies, Inc. All the reagents were obtained from Sigma-Aldrich Chemical Co., Wako Pure Chemical Industries, Ltd., and

Tokyo Chemical Industry Co., Ltd., and were used as received, unless otherwise specified.

Equipment. UV−vis−NIR absorption spectra were recorded on a UV-3100PC scanning spectrophotometer (Shimadzu Co.). Photoluminescence spectra were measured on a NIR-PL system (Shimadzu Co.). Circular dichroism spectra were recorded on a J-600 spectropolarimeter (JASCO International Co. Ltd.). ^{1}H NMR analysis (270 MHz), ESI-MS measurement, and elemental analysis were performed on a JEOL JNM-EX270 spectrometer, LCQ Fleet (Thermo Scientific), and a VarioMICRO-cube (Elementar Analysensysteme GmbH), respectively. Centrifugation was carried out with Beckman Avanti J-E, Optima-TL, and L-70. Tip-sonication was performed with MISONIX (120 W, 20 kHz).

Synthesis of Chiral Diporphyrin (*R*)-1. 3,6-Bis(4,4,5,5,-tetramethyl-1,3,2-dioxaborolan-2-yl)-9,10-dioctyloxyphenanthrene (13.7 mg, 0.020 mmol),[39] 5-bromo-10,20-di(1′-*tert*-butoxycarbonylamino-2′-phenylethyl)-(*R*)-porphinatozinc(II) (35.7 mg, 0.040 mmol),[30] Cs_2CO_3 (39 mg, 0.12 mmol), and $Pd(PPh_3)_4$ (2.3 mg, 0.0020 mmol) were dissolved in a mixture of dry DMF (2.0 mL) and dry toluene (2.0 mL). The solution was stirred at 85 °C for 5 h under Ar. After the addition of water, the product was extracted with dichloromethane. The extract was dried over anhydrous $MgSO_4$, passed through a short silica gel column, and concentrated. The residue was subjected to recycling preparative GPC-HPLC (LC-908, Japan Analytical Industry Co., Ltd.) to give chiral diporphyrin (*R*)-**1** as a purple solid (31.2 mg, 81% yield). Anal. Calcd for $C_{122}H_{130}N_{12}O_{10}Zn_2$: C, 71.30; H, 6.38; N, 8.18. Found: C, 71.08; H, 6.39; N, 8.11. UV−vis (MeOH): λ_{max}: 414, 426, 549, and 585 nm. Fluorescence (MeOH, λ_{ex} = 414 nm); λ_{max} = 596, 644 nm.

Because decent spectra of ^{1}H NMR and ESI-MS of the zinc diporphyrin **1** were not obtained, the corresponding free base diporphyrin was prepared by the acid treatment of **1** and subjected to analyses. ESI-MS: Calcd for $C_{122}H_{135}N_{12}O_{10}$ [$(M + H)^+$]: 1927.8. Found: 1929.0; [$(M + 2H)^{2+}$]: 965.02. Found: 964.8. The spectrum is shown in Figure S2 in the Supporting Information. ^{1}H NMR (DMSO-d_6, 270 MHz): δ 10.18 (s, 2H, meso-H), 9.64 (4H, β-H), 9.42 (4H, β-H), 8.83 (2H, phenanthrene ring), 8.75 (4H, β-H), 8.72 (4H, β-H), 8.59 (4H, phenanthrene ring), 7.20 (4H, C*H*CH$_2$Ph), 6.89−7.13 (m, 20H, phenyl), 4.59 (4H, OC*H*$_2$CH$_2$CH$_2$), 3.73−4.05 (8H, CHC*H*$_2$Ph), 2.12 (4H, OCH$_2$C*H*$_2$CH$_2$), 1.75 (4H, OCH$_2$CH$_2$C*H*$_2$), 1.33−1.40 (m, 16H), 1.33 (s, 18H, *tert*-butyl), 1.06 (s, 18H, *tert*-butyl), 0.87 (6H, CH_3), 0.34 (4H, NH), −3.13 (s, 4H, NH of pyrrole). The spectrum is shown in Figure S3 in the Supporting Information.

The chiral diporphyrin (*S*)-**1** was synthesized similarly by use of 5-bromo-10,20-bis(1′-*tert*-butoxycarbonylamino-2′-phenylethyl)-(*S*)-porphinatozinc(II) and identified in a similar manner.

Extraction of CoMoCAT−SWNTs with 1. CoMoCAT (10 mg) and (*R*)- or (*S*)-**1** (10 mg) in methanol (40 mL) were bath-sonicated at 20 °C for 16 h. After the resulting suspension was centrifuged at 50400*g* for 3 h, the supernatant was subjected to UV−vis−NIR and CD measurements (Figure S1). After concentration of the supernatant, the residue was washed with pyridine and THF several times until the porphyrin Soret band disappeared in the UV−vis spectra of the washings. The thoroughly washed SWNTs were analyzed with Raman spectroscopy at excitations of 633 nm (Figure 2b) and 488 nm (Figure 3). The solid sample was dispersed into D_2O (18.5 mL) in the presence of SDBS (10 mg/mL) by tip-type ultrasonication for 40 min for CoMoCAT and for 3 h for the SWNTs extracted with **1**. After centrifugation (543 000*g*, 70 min for CoMoCAT or 136 000*g*, 20 min for the extracted SWNTs), the upper layer (∼75%) of the supernatant was subjected to vis-NIR (Figure 2a), PL (Figure 2c), and CD measurements (Figure 4).

Acknowledgment. We thank Professor Hiroshi Imahori (Kyoto University) for allowing us to use the PL spectrophotometer, Professor Tetsuo Ishida (Shiga University of Medical Science) for analyzing **1** with ESI-MS spectroscopy, and Professors R. Bruce Weisman and Sergei M. Bachilo (Rice University) for helpful discussions. This work was financially supported by Grant-in-Aid for Scientific Research on Priority Areas (No. 20048003 and No. 20048004), Grant-in-Aid for Scientific Research (B) (No. 20350064 and No. 20340075), and Industrial Technology Research Grant Program in 2005 from New Energy and Industrial Technology Development Organisation (NEDO) of Japan. A.F.M.M.R. acknowledges Japan Society of Promotion of Science (JSPS) for providing him postdoctoral fellowship (No. 2008350).

Supporting Information Available: Figures S1−S3. This material is available free of charge via the Internet at http://pubs.acs.org.

JA1044677

(39) Vanormelingen, W.; Smeets, A.; Franz, E.; Asselberghs, I.; Clays, K.; Verbiest, T.; Koeckelberghs, G. *Macromolecules* **2009**, *42*, 4282–4287.